



Experimental estimation and numerical optimization of 'cylindricity' error in flow forming of H30 aluminium alloy tubes

Tarak Nath De¹ · Bikramjit Podder² · Nirmal Baran Hui³ · Chandan Mondal⁴ Received: 27 October 2020 / Accepted: 22 December 2020 / Published online: 18 January 2021
© The Author(s) 2021

Abstract

The present article analyses the influence of flow forming input parameters on the development of "cylindricity error" in H30 aluminum alloy seamless tubes fabricated by a single pass reverse flow forming process. Measurement and control of geometrical precision in terms of cylindricity encompassing straightness and roundness are critical for the success of component manufacturing by flow forming. The experimental trials with a predefined range of input parameters conforming to the full factorial design of experiments approach have been performed, and corresponding cylindricity data have been recorded as the outcome. An empirical relation has been established between the input parameters and the cylindricity. It has been established that cylindricity value increases sharply with an increase in axial stagger contributing 39% to the outcome, whereas the percentage contributions of in-feed and feed-speed ratio are found to be less than 1%. The adequacy of the proposed model has further been analyzed and validated through the confirmation tests. In order to obtain better control over the overall process towards achieving higher productivity and accuracy, 2 meta-heuristic optimization algorithms namely, teaching and learning-based algorithm and genetic algorithm have been utilized for optimization of input process parameters to minimize cylindricity error. Both the algorithms predict that a combination of higher feed rate and lower value of axial stagger and in-feed parameters is essential to achieve the lowest cylindricity error in H30 Al alloy. Confirmatory experimental trials have been carried out to validate both the regression model and optimization, and have been found to agree well with the model predictions described herein.

Keywords Flow forming · Cylindricity · Laser tracker · TLBO · Genetic algorithm · ANOVA

1 Introduction

Flow-forming is the preferred process for the realization of thin-walled cylindrical products requiring a high degree of geometrical precision. In this process, the inner diameter of the cylinder remains constant, but length increases by reduction of thickness. The generic overview of the flow forming process and influence of various input parameters are described in detail by Kalpakjian et al. [1]. Among the

several controlling parameters the speed of the spindle, axial feed, in-feed/thickness reduction (IF), axial stagger (AS), and roller geometry are considered to be the most significant parameters that determine the quality of the product. Jiang et al. [2] have proposed an accurate and efficient methodology to evaluate the cylindricity error. Alrazzaq et al. [3] have carried out an experimental investigation on geometrical accuracy for the metal spinning process and established a relation between spinning

Supplementary Information The online version contains supplementary material available at (<https://doi.org/10.1007/s42452-020-04074-2>)

✉ Chandan Mondal, chandan_mondal@yahoo.com | ¹Advanced Systems Laboratory (ASL), Hyderabad 500058, India. ²Defence Research and Development Laboratory (DRDL), Hyderabad 500058, India. ³National Institute of Technology, Durgapur, West Bengal 713209, India. ⁴Defence Metallurgical Research Laboratory (DMRL), P.O.-Kanchanbagh, Hyderabad 500058, India.

SN Applied Sciences (2021) 3:150 | <https://doi.org/10.1007/s42452-020-04074-2>

parameters and roundness. Analysis and validation of the phenomenon of diametrical growth with the change in input parameters have been attempted by Fong et al. [4]. Davidson et al. [5] have carried out a detailed study on flow-formed aluminum tubes to establish a relation between the qualities of the tube with a change in input parameters. Ebrahimi et al. [6], on other hand, have studied the quality of surface, dimensional accuracy, and mechanical properties of flow-formed titanium tubes. The effects of input parameter on the ovality, internal diameter, and spring back of flow formed AA6082 aluminum alloy tubes have been examined by Podder et al. [7]. Conventionally, a meta-heuristic search algorithm called the genetic algorithm (GA) has widely been applied to optimization related problems due to its robustness and flexibility [8]. Deb et al. have explained the power of GA in tackling real-parameter optimization problems [8]. Recently, a new algorithm called the teaching learning-based optimization algorithm (TLBO) for optimization of process parameters for multi-pass turning has been proposed by Venkata Rao and co-workers [9]. It has been claimed that the method can be used generically to solve several optimization problems and it yields a better result with lesser computational load and time.

From the aforementioned discussion, it is amply clear that the input parameters play an important role in determining the geometry of the final formed products [10]. Although there is a large body of literature on the subject, deliberations on the overall geometrical precision of the formed tube are rather scarce in the open literature. A flow formed product with minimum diametrical growth and higher ovality or vice-versa cannot be considered as a precision tube. Optimization of one individual parameter may improve some of the output parameters, but simultaneously it may deteriorate some different output parameters. The interdependency of the response parameters further adds to the complexity of the problem. Quality of flow-forming is largely dependent on the accuracy of the formed cylinder. The geometrical accuracy of the flow-formed product can be defined with a single parameter i.e., "cylindricity". Cylindricity is a three-dimensional geometrical tolerance that defines the form of the cylindrical feature. Cylindricity error encompasses the combined inaccuracies due to straightness and roundness error. Controlling the cylindricity error by controlling the level of input parameters is therefore a work of prime importance to meet the challenges of high geometrical accuracy. In the present article, three input parameters are systematically varied, and their effects on cylindricity have been measured and a generic mathematical relation has been generated to establish the relation between cylindricity and input variables. Further, two meta-heuristic optimization algorithms namely, teaching and learning based algorithm

(TLBO) and genetic algorithm (GA) are utilized to achieve the optimum level of input variables for attaining the minimum cylindricity error. Optimization results of both the algorithms are compared and validated with respect to the experimental result.

It is the purpose of the present study to optimize the processing parameter in order to minimize the cylindricity error during the flow forming of the AA6082 Al alloy tube. The experimental values of cylindricity error have been obtained within a predetermined range of parameters conforming to the full factorial DOE and a mathematical relationship is established based on a statistical analysis of experimental results. Two meta-heuristic optimization algorithms have been applied to the developed model and the optimum levels of processing parameters have been achieved. The validity of the optimized processing parameters has been well corroborated by experimentation and thus, provides valuable guidance for bulk production.

2 Experimental procedure

Flow forming trials for the present study were performed in a three-roller CNC machine (make: Leifield). A previously-optimized range of processing parameters was utilized for forming trials [7], and in all the cases, the required reduction in thickness was achieved in a single pass keeping in mind the productivity of flow-formed tubes. Consequently, the number of forming passes was not considered as an input variable during the experimentation. The reverse flow forming process was adapted, and the industrially accepted roller geometry and roller combinations have been used for the present testing (Fig. 1a). The process details and the specification of the machine are reported elsewhere [11]. The tools used for the experiment were mandrel assembly, toothed ring, and stripper ring. The inner diameter of the preform was machined so as to fit the outer diameter mandrel with suitable clearance. The preform was mounted on the mandrel with the help of a toothed ring and stripper ring. The toothed ring and stripper ring were assembled to the mandrel by keyway and the typical assembly set up is shown in Fig. 1b. The deformation of the preform was carried out with the hydraulically operated rollers that were symmetrically placed at 120° apart. All three rollers were staggered both axially and radially to avoid overlapping of the deformation zone. Quality of flow forming depends on mainly three factors viz., preform material condition, roller geometry, and machine setting [1, 12]. The present study focuses on 4 main machine setting parameters i.e. feed, mandrel speed, axial stagger (AS) of rollers, and in-feed (IF) for a given preform material and roller geometry. The ratio of feed and speed or feed rate gives the axial

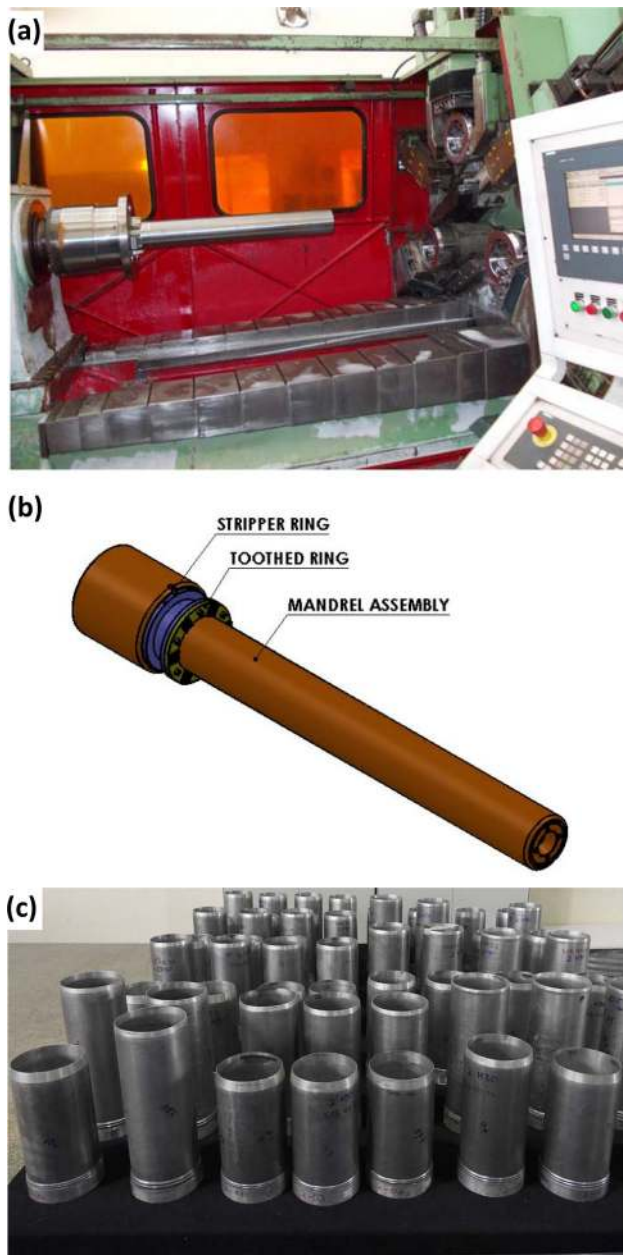


Fig. 1 **a** Photograph of flow forming machine, **b** mandrel assembly, **c** flow formed tubes produced using the range of processing parameters

movement of rollers which is a more practical parameter for rotary forming processes. This ratio was considered as the feed speed ratio (FS) in the present study. All the three parameters were varied at 4 levels within a feasible range of flow forming without defects. According to the design of experiment (DOE) concept, a full factorial design comprising of 4^3 (i.e., 64) components has been considered. Consequently, three selected input parameters, i.e., feed speed ratio, axial stagger, and in-feed, were taken into consideration at 4 equal levels of variations. The lower and

Table 1 Input variables and their levels of variations

Input	Level-1	Level-2	Level-3	Level-4
Feed Speed Ratio (FS)	0.5	0.6	0.7	0.8
Axial Stagger (AS)	9.5	11.0	12.5	14.0
Infeed (IF)	3.0	3.5	4.0	4.5

upper limits of the independent variables for the present study are shown in Table 1. Following the matrix of input parameters, 64 numbers of flow formed tubes were produced (Fig. 1c). For each flow formed tube so produced, the inner surface cylindricity was measured with the help of portable CMM (Laser Tracker).

2.1 'Preform' material

H30 (equivalent to AA6082) aluminum alloy was used as 'preform' material for the present study. The analyzed chemical composition of the preform material (wt.% of constituent elements) and mechanical properties are given in Tables 2 and 3, respectively. Flow forming was carried out in the solution annealed condition. In order to counter any unintentional distortion due to solution annealing operation, a 2 mm finish-machining allowance was been maintained for all the preform material. Following the solution treatment and water quenching, the 'preform' was immediately transferred to a freezer at 4 °C to minimize the effect of natural aging. Subsequently, finish machining operation was carried out on the preforms before they were subjected to forming trials. A schematic diagram of the pre-form is shown in Fig. 2. A strict process sequence has been maintained to ensure a uniform time gap of 48 h between solution annealing and flow forming.

2.2 Cylindricity measurement methodology

Cylindricity is the three-dimensional geometrical tolerance that defines the form of a cylindrical feature. It encompasses both the roundness and straightness of a cylinder along its axis. The definition of cylindricity has been clearly explained in standard ASME Y 14.5 [13]. For the present study, cylindricity was measured using a portable CMM laser tracker. The laser tracker is a polar-based measurement system. Laser tracker measures a point in 3D space by measuring the azimuth (θ), elevation (Φ) angles, and distance (R). The angle and distance data are converted into X, Y, Z Cartesian coordinates as: $x=r(\sin\theta \cdot \cos\Phi)$, $y=r(\sin\theta \cdot \sin\Phi)$, $z=r \cdot \cos\Phi$. The distance measurement was carried out using an interferometer (IFM) and an absolute distance meter (ADM) devices. Incremental distance measurement is made within an interferometer. A stabilized, helium–neon laser is divided into 2 beams.

Table 2 Chemical composition of H30 aluminium alloy

Constituent	Si	Mg	Mn	Fe	Cu	Al
Wt%	0.96	0.6	0.57	0.24	0.008	balance

Table 3 Mechanical properties of Preform

Yield Strength	Tensile Strength	% Elongation	Hardness
163 ± 4 MPa	285 ± 3 MPa	30 ± 2	105 ± 5 VHN

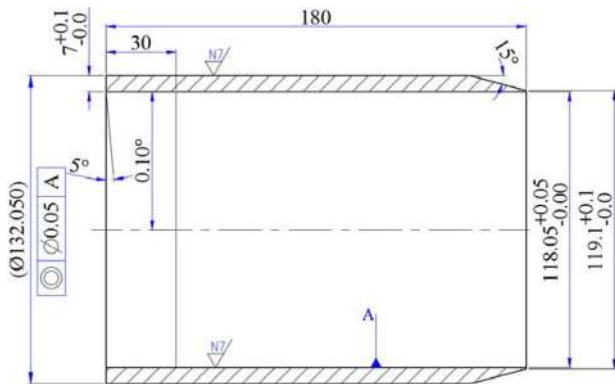


Fig. 2 Sketch of a pre-form with dimensions

One beam moves directly into the interferometer and the other one comes out of the system and reflects off the corner cube reflector (CCR) and back into the interferometer. The CCR has three mirror surfaces meeting at right angles to each other like a corner of the cube with a pivot. Interference takes place between 2 beams having the same frequency, but there exists a phase difference between 2 beams because of the difference in distance traveled by them. Two beams interfere inside the interferometer and result in a cyclic change each time the CCR moves by a distance equal to one-fourth of the wavelength of the light (~0.16 μm). The counter counts the number of cyclic changes to evaluate the distance traveled. Since the wavelength of the helium–neon laser is 633 nm, a very finer resolution of one-quarter of the wavelength (i.e., ~0.16 μm) can be achieved.

The length is checked for both 0.5" and 1.5" reflectors using both the IFM and ADM. If the difference between the specified length and measured length is more than the specified limit, then the instrument is recalibrated. The calibration is done for the qualification of the system before measurement. Calibration of both the IFM and ADM equipment was done for the system qualification for an actual measurement. The invar scale bar was checked for its length before starting the measurement. Coordinates of points spreading on the cylindrical object surface were

collected with the CCR. The best fit cylinder was derived by the least square method considering the coordinates of the points of the object [14]. A Leica laser tracker (model Ltd 840) was used for the present study. The Metrolog XG (V 8.001) software was used for fitting the best fit cylinder of more than a hundred data points captured on the surface of the cylinder. The radial distance of the best fit cylinder axis for minimum point and maximum point on the surface has been reported as 'cylindricity' value. Cylindricity of the mandrel used for flow forming has been measured as 0.052 mm. The measurement setup is shown in Fig. 3.

2.3 Regression model

The flow forming trials have been designed based on full factorial DOE having 3 factors, and 4 levels for each factor. Hence, a total number of 64 (= 4³) experiments have been carried out. The cylindricity value for each tube is measured as a response parameter after each forming operation. The response parameter is expressed as a function of the independent variable, as shown in Eq. (1). Cylindricity is expressed in terms of individual variables and their interaction terms. A mathematical relation has been established by finding out the values of all constants i.e., a₀ to a₇ of Eq. (2). For each term of independent variables, significance tests have been carried out using ANOVA.

$$Y = f(X_1, X_2, X_3) \tag{1}$$

$$Y = a_0 + a_1X_1 + a_2X_2 + a_3X_3 + a_4X_1 \cdot X_2 + a_5X_2 \cdot X_3 + a_6X_1 \cdot X_3 + a_7X_1 \cdot X_2 \cdot X_3 \tag{2}$$

2.4 Teaching learning based algorithm

Teaching learning based algorithm (TLBO) is a heuristic search algorithm specific to a problem. TLBO is proposed by Rao et al. [15]. TLBO needs only the size of the population and generation number for execution. Rao [16] has successfully implemented the algorithm for several mechanical optimization problems. The algorithm can solve both constrained and unconstrained problems. One major advantage of TLBO is that it does not require any parameters to be controlled during its execution. Besides, it has a higher degree of repeatability. To obtain a global solution for a continuous non-linear function,

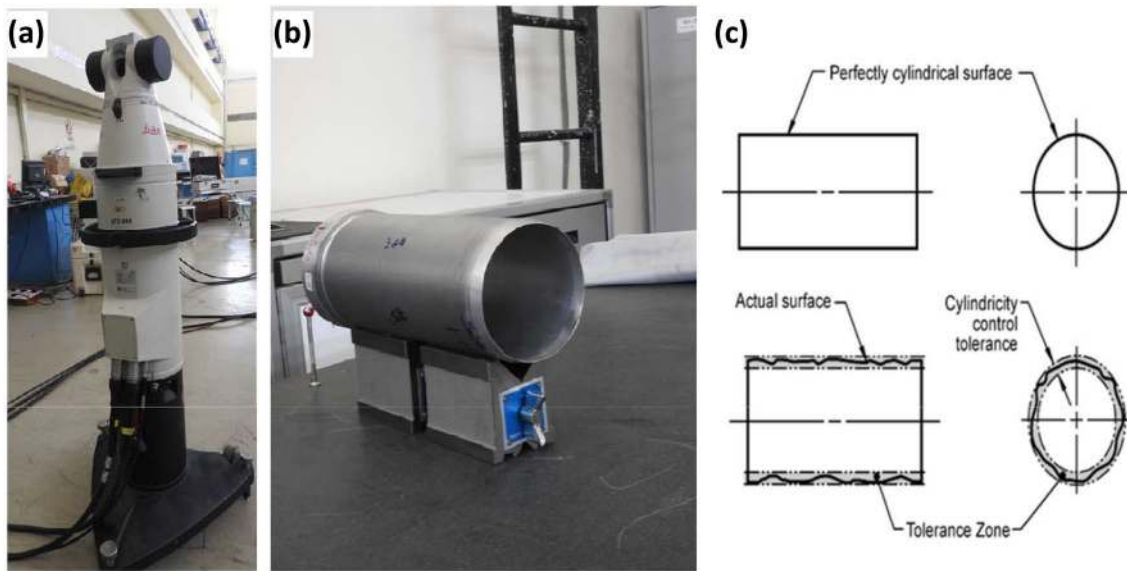


Fig. 3 Cylindricity measurement set up: **a** laser tracker, **b** flow formed tube, **c** schematic representation of cylindricity

the algorithm calls for a relatively reduced computational load. This is based on the traditional teaching–learning phenomena of a class for reaching the optimum point. Here, the initial population is a group of students. Different input variables are considered as the different subjects of the students. The result scored by the student is assumed as the value of fitness. The teacher is decided based on the best solution among the population. This algorithm consists of two major phases: (a) teaching phase, and (b) learner phase.

2.4.1 Teaching phase

Here, the teacher tries to increase the knowledge of the student to a particular level for the subject which he/she is teaching. The teacher cannot enhance the knowledge of the students to the desired level. So, the teacher makes an effort to enhance the mean level of knowledge of the population. The best knowledgeable person of the population is considered a teacher. At any iteration, i , ‘ m ’ is considered as the number of subjects i.e., input variables, and ‘ n ’ is the number of learners i.e. population size. Here, the population size ‘ k ’ varies from 1 to n . $M_{i,j}$ is the mean result for a particular subject ‘ j ’ ($j = 1, 2, 3, \dots, m$) of the population. $X_{total-kbest,i}$ is the overall best result considering all subjects. Considering the teacher as the most knowledgeable person of the population, $X_{total-kbest,i}$ is considered as the teacher. The solution is modified by the difference between the existing mean for each subject the corresponding result of the teacher. It is expressed in Eq. (3).

$$\text{Difference_Mean}_{j,k,i} = ri(X_{j,kbest,i} - T_F M_{j,i}) \tag{3}$$

Here, $X_{j,kbest,i}$ is the result of the teacher in subject ‘ j ’ and r_i is the random number within 0 to 1. The teaching factor (T_F) decides the change in the mean. T_F is either 1 or 2. T_F is taken randomly and shown in Eq. (4). T_F may be decided by the program randomly. It has been found that for a value of $T_F = 1$ or 2, the algorithm gives a better result [16]. T_F is not to be considered as a parameter in the TLBO algorithm. It is one of the steps.

$$T_F = \text{round}[1 + \text{rand}(0, 1)\{2 - 1\}] \tag{4}$$

Considering the value of $\text{Difference_Mean}_{j,k,i}$, the exiting solution is changed as per Eq. (5). Here, $X'_{j,k,i}$ is the updated value of $X_{j,k,i}$. $X'_{j,k,i}$ which is to be considered if it yields a better result. Accepted values of the teacher phase are saved and used as initial values to the learner phase.

$$X'_{j,k,i} = X_{j,k,i} + \text{Difference_Mean}_{j,k,i} \tag{5}$$

2.4.2 Learner phase

Students may learn either from the teacher or by interacting among themselves. In this phase, learners interact with themselves randomly. Generally, the learner learns from the other learner who is having better knowledge. Learner P and Q interact within themselves for the population size (n). This phase of P and Q is shown in Eqs. (6) and (7) for minimization function and Eqs. (8) and (9) for a maximization problem. For both the cases $X'_{total-P,i} \neq X'_{total-Q,i}$.

For minimization problem:

$$X''_{j,P,i} = X'_{j,P,i} + r_i(X'_{j,P,i} - X'_{j,Q,i}) \text{ if } X'_{\text{total}-P,i} < X'_{\text{total}-Q,i} \quad (6)$$

$$X''_{j,P,i} = X'_{j,P,i} + r_i(X'_{j,Q,i} - X'_{j,P,i}) \text{ if } X'_{\text{total}-Q,i} < X'_{\text{total}-P,i} \quad (7)$$

For maximization problem:

$$X''_{j,P,i} = X'_{j,P,i} + r_i(X'_{j,P,i} - X'_{j,Q,i}) \text{ if } X'_{\text{total}-P,i} > X'_{\text{total}-Q,i} \quad (8)$$

$$X''_{j,P,i} = X'_{j,P,i} + r_i(X'_{j,Q,i} - X'_{j,P,i}) \text{ if } X'_{\text{total}-Q,i} > X'_{\text{total}-P,i} \quad (9)$$

2.4.3 Steps for TLBO

- Obtaining the optimization function
- Defining the size of the population
- Generating the population
- The identification of teacher (best in the population)
- Updating the learner considering the knowledge of the teacher
- Calculating the objective function of the new learner
- Comparing the new and initial population and select the better one to get a new population
- Using the new population as the input to the learner phase
- Learners' interaction randomly to upgrade their knowledge
- New population generation by interaction
- Comparing the outputs with the output of the teacher phase
- Selection of better one to generate a new population
- Using a new population as an input to the next generation as an initial population
- Repeating above steps until the specified number of generation is reached.

2.5 Genetic algorithm

Genetic Algorithm (GA) is a meta-heuristic search technique that deploys a higher strategy level for controlling a lower level in the algorithm. The concept of GA is inspired by nature. GA mimics the concept of Darwin's natural evolution theory. The search methodology is very robust and flexible [17]. The required solution is modeled as a fitness function. The optimization of the objective function is carried out by finding suitable values of input variables. Next-generation is formed by genetic operators (viz., cross-over, and mutation). Variables are taken in the form of a *chromosome*. Sub-string is a combination of various parameters. The values of input variables are considered as Genes in the sub-string [17]. There are six modules in GA as shown

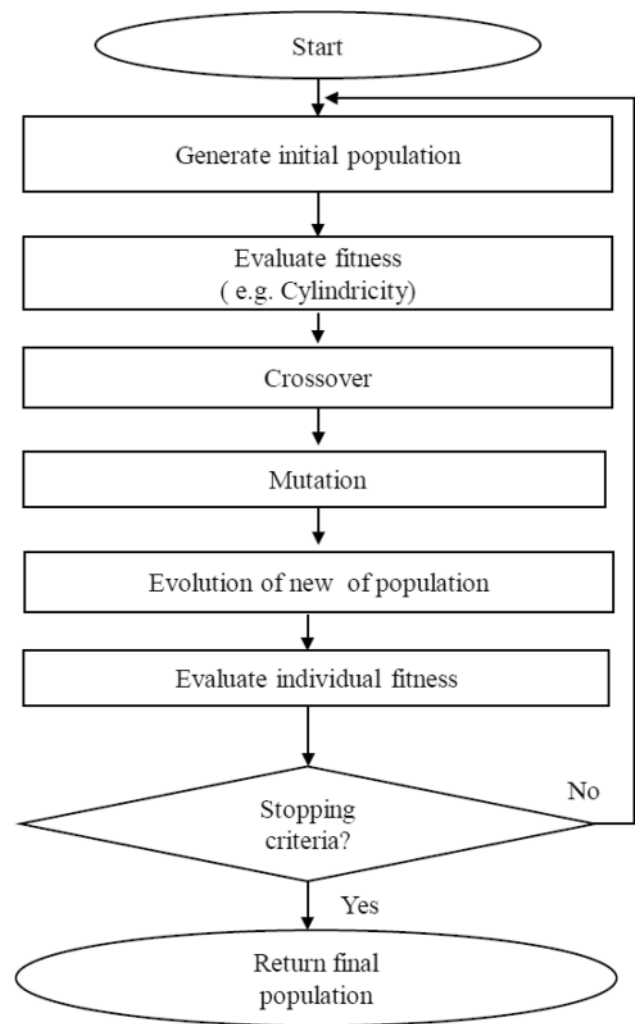


Fig. 4 A flow-chart showing steps of genetic algorithm

in Fig.4. The highest rank *chromosome* of the population is selected. In the cross-over process, the exchange of desirable qualities between parents occurs. In this stage, the random cutting of *chromosomes* is done, and substrings are exchanged. The cross-over offsprings are taken into mutation operation. After reaching the termination criteria, the optimized result is displayed. The optimization tool of MATLAB software is used to solve the present problem.

3 Results and discussion

The aim of the present study is to estimate the constants of Eq. (2) using experimental data through the full-factorial design of experiments. An empirical model has been developed between 3 input variables and one response variable. The analysis of variance (ANOVA) is performed to evaluate the model adequacy for the correlation of

cylindricity error with input variables. For each term of independent variables, significance tests have been carried out using ANOVA. The model summary statistics and associated fit summary for cylindricity measurements for the model are shown in Table 4. The significance of all input terms and their interactions as proposed in the model has been evaluated out by the 'P-test'. Furthermore, the so-called 'F-test' is also carried out to rule out the null hypothesis. R^2 and R^2 -adj values are also tabulated to

ascertain the fit of the present model. The regression equation of cylindricity with FS, AS, and IF is given in Eq. (10). The percentage contribution (PC) of each input parameter and their interaction terms are also tabulated to understand the sensitivity of the input parameter on cylindricity. The residual plots of the model are shown in Fig.5. Surface plots for input variables and cylindricity are shown in Fig. 6. Plots for main effect and interaction terms in the model are shown in Figs.7 and 8, respectively. MINITAB

Table 4 Regression model summary statistics evaluated by ANOVA

Source	DF	SEQ SS	C ontribution (%)	ADJ-SS	ADJ-MS	F-VAL	p-VAL
Regression	7	0.203194	90.51	0.20319	0.029028	76.32	0.0000
FS	1	0.000846	0.38	0.02670	0.026698	70.20	0.0000
AS	1	0.087848	39.13	0.02316	0.023159	60.89	0.0000
IF	1	0.000017	0.01	0.02198	0.021977	57.78	0.0000
FS*AS	1	0.059341	26.43	0.02002	0.020020	52.64	0.0000
FS*IF	1	0.029316	13.06	0.01686	0.016865	44.34	0.0000
AS*IF	1	0.014432	6.43	0.01577	0.015766	41.45	0.0000
FS*AS*IF	1	0.011394	5.08	0.01139	0.011394	29.96	0.000001
Error	56	0.021298	9.49	0.02130	0.000380		
Total	63	0.224493	100.00				

$R^2 = 90.51\%$, R^2 (adj) = 89.33%

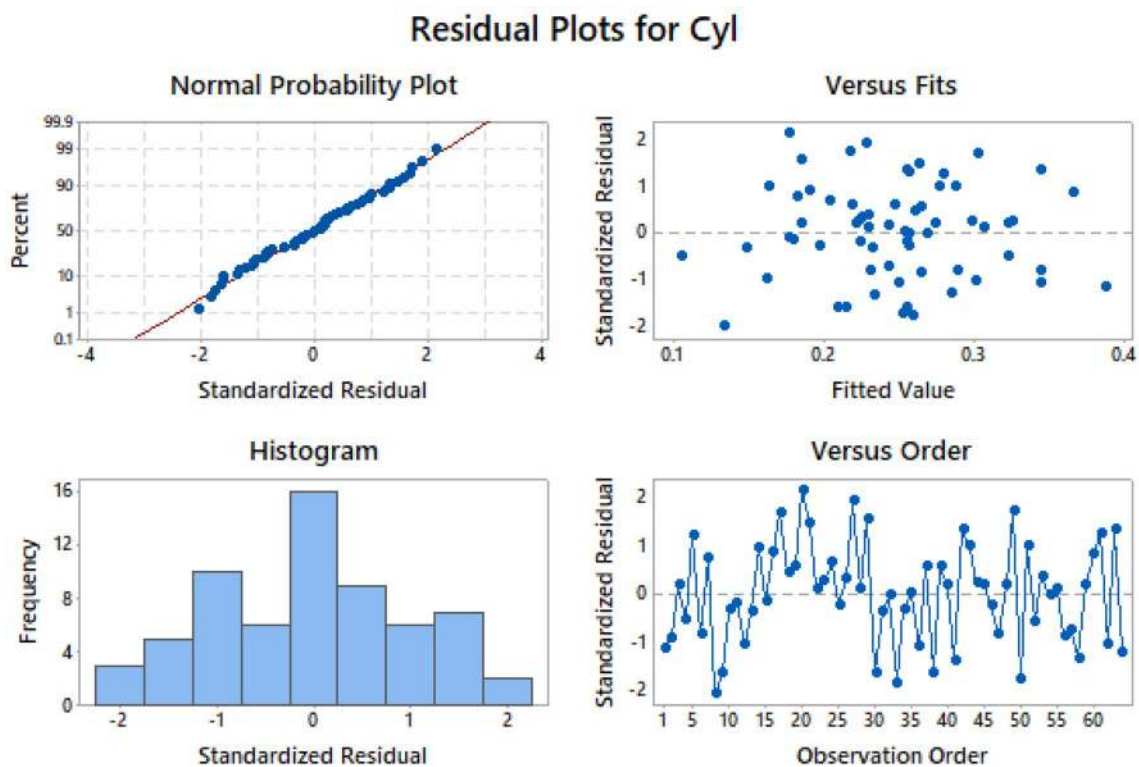


Fig. 5 Residual plots of cylindricity

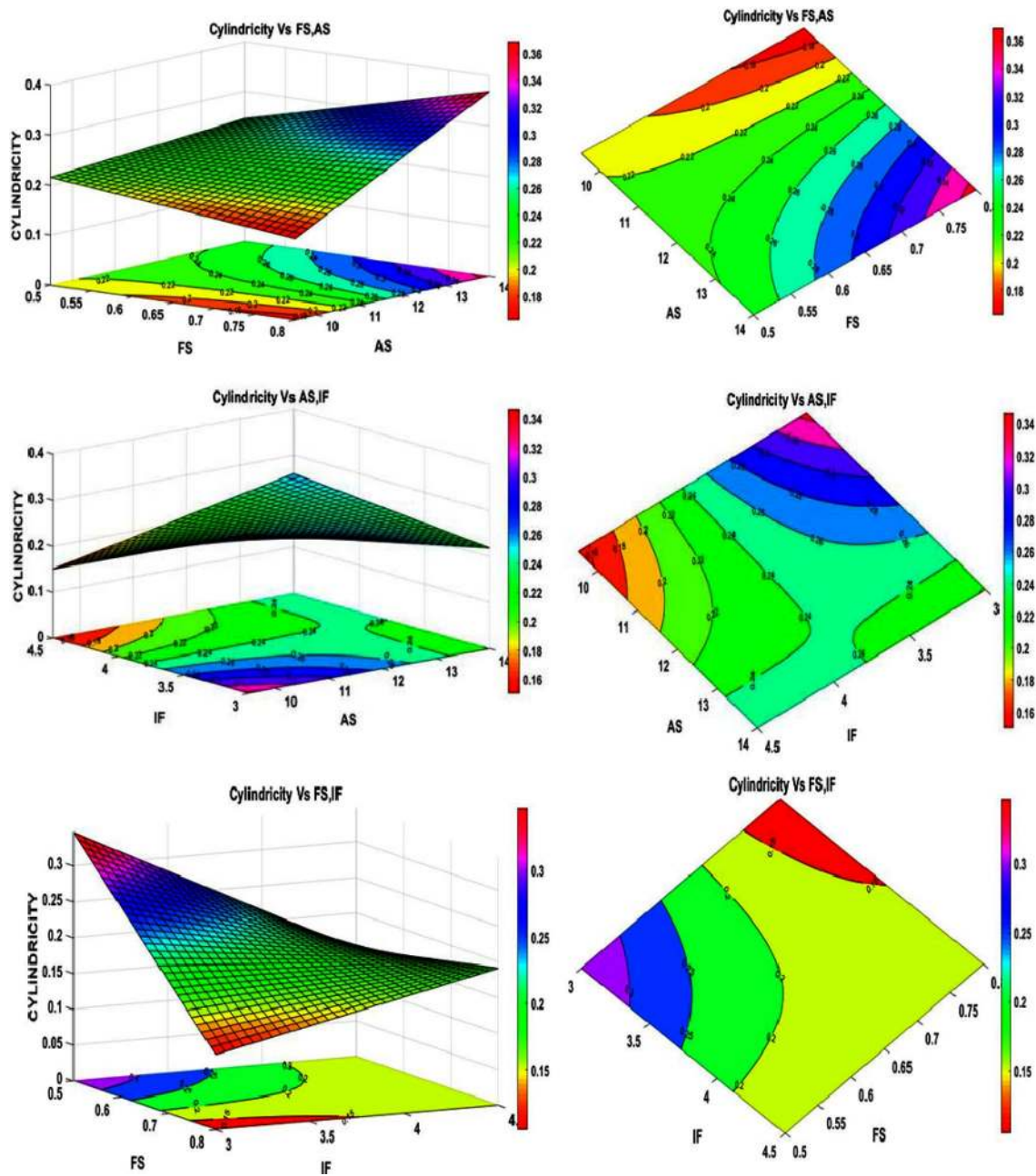


Fig. 6 Surface plots for the input variables

software is used to solve the present problem. The regression equation for cylindricity error as a function of input variables is given in Eq. (10).

$$CYL = 6.39 - 8.77FS - 0.453AS - 1.38IF + 0.64FS * AS + 1.84FS * IF + 0.09AS * IF - 0.12FS * AS * IF \tag{10}$$

The empirical model as described by Eq. (10) has been developed through experimentally measured cylindricity values corresponding to the 3 input variables with

predefined levels conforming to the full factorial DOE approach (the complete dataset has been provided as supplementary data). To summarize the test for significance

on individual model co-efficient, the model adequacy is further considered through ANOVA. The result of the 'P-test' shows that $p < 0.05$ for all individual terms and their interaction, which confirms the significance of all terms in

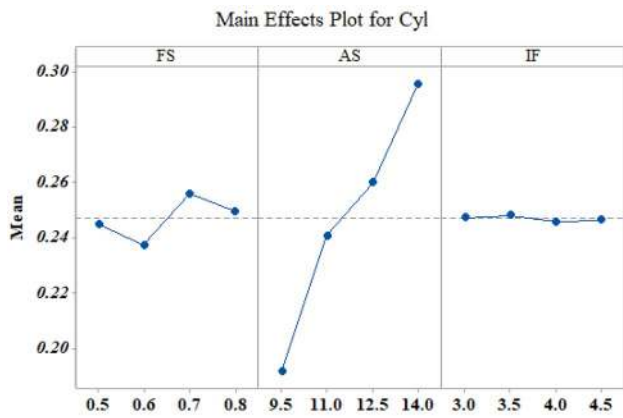


Fig. 7 Main effect plots of the model

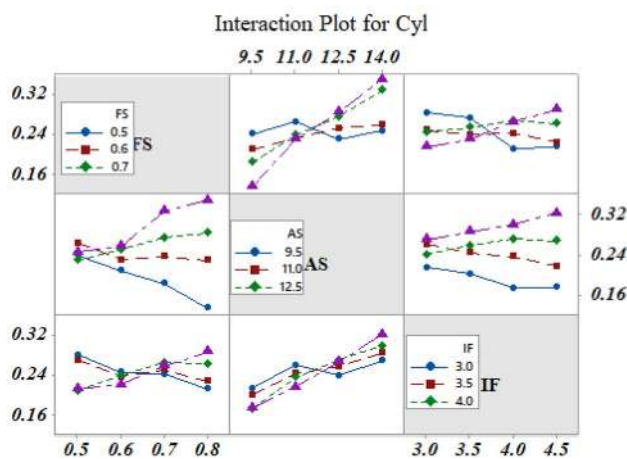


Fig. 8 Interaction effect plot of the model

the model. From the 'F-test', it is evident that the value of $F > 10$ for all cases and thus, the null hypothesis nullified. The value R^2 reflects the correspondence between input and output variables. The value is R^2 (90.51% i.e., close to unity) implies a better fitness of the model. It is generally believed that the model fits better with actual data when the R^2 value approaches unity [18]. However, it is worth considering the fact that the value of R^2 also increases with the increase in independent variables in the model. So, strictly speaking, a higher value of R^2 does not always necessarily indicate a better fit of the model. The precision of the regression model can be enhanced by adjusting the coefficient of determination (R^2) value for the degrees of freedom. R^2 (adj.) meets this purpose by comparing residuals per unit degree of freedom. Therefore, R^2 (adj.) is further evaluated and compared with R^2 . For the present problem, the difference between R^2 and R^2 -adj is only 1.18%. This confirms that all of the significant terms are available in the model. As shown in Fig. 5, the residuals lie in normal

lines in the plot. The residuals do not exhibit any particular pattern. It confirms that there is no measurement error during the collection of data. The main effect plot in Fig. 7 indicates that the cylindricity error becomes higher with an increase in AS, but with FS, it increases marginally from 0.6 to 0.7 and decreases for initial and end phases. The main effect plot further shows that there is a marginal change in the cylindricity value with thickness reduction (IF). The interaction plot as displayed in Fig. 8 exhibits that the cylindricity value increases with interaction terms AS-FS and AS-IF, but change is marginal for FS-IF. The surface plots in Fig. 6 shows the complex contour of variations in the cylindricity with the employed range of input variables. Surface plots show that cylindricity errors hardly changes with change in the in-feed levels, but it increases significantly with axial stagger. The feed speed ratio has a mixed effect on cylindricity error. The percentage contribution of input parameters and the interaction terms for cylindricity error has been tabulated in Table 4. It is evident from the analyses of the results that the axial stagger is the most influential parameter, which contributes 39%. On the contrary, both feed-speed ratio and in-feed evolve as relatively less significant parameters regarding control of cylindricity value. The percentage contributions of interaction parameters (AS*FS, FS*IF, and AS*IF) are estimated to be 26%, 13%, and 6.43%, respectively. However, among all the interaction parameters, the more significant ones contain axial stagger and it reinforces the axial stagger as the dominant input parameter in the present case.

Optimization is carried out with both TLBO and GA concepts. Several iterations are performed with a different combination of population size and generation. The best among them are reported here. The range of the output of TLBO varies significantly for several iterations, but

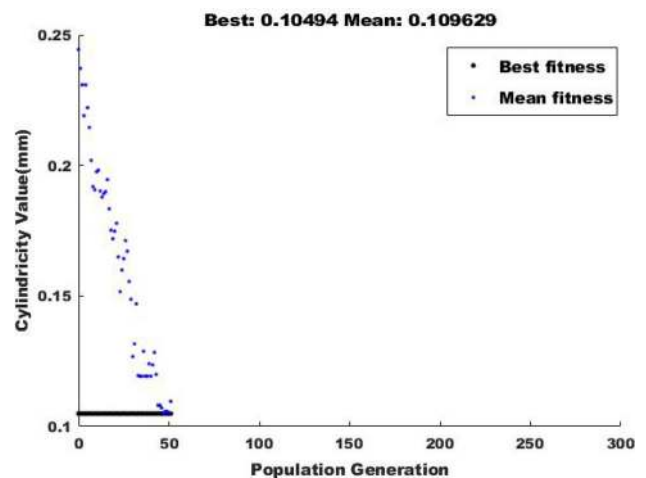


Fig. 9 Convergence graph for minimization of cylindricity error by genetic algorithm

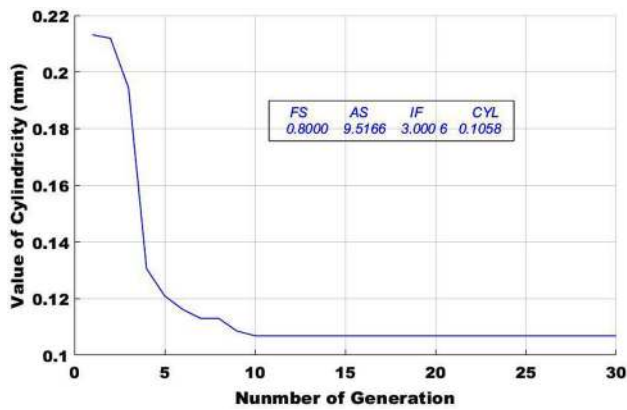


Fig. 10 Convergence graph for minimization of cylindricity error by TLBO algorithm

GA produces results with almost the same values for the number of iterations. The optimization result of GA and TLBO are shown in Figs.9 and 10, respectively. The output levels for both the optimization algorithms are similar. However, GA provides a marginally better result for the present problem.

From the aforementioned analyses, it is rather interesting to note the differential effects of the input parameters on the development of cylindricity error. Notwithstanding the dominance of the axial stagger on the cylindricity as demonstrated by regression analysis, two heuristic- algorithm based optimization techniques insist that a combination of higher feed rate and lower value of axial stagger and in-feed parameters is essential to achieve the lowest cylindricity error. A mechanistic appraisal is therefore attempted. It is generally believed that the cylindricity of flow formed tube originates from the tolerance (gap) between the inner diameter of the preform and the outer diameter of the mandrel. In order to eliminate the possible interference of such unavoidable operational necessity, a constant tolerance of 50 μm has been maintained between the preform and mandrel for the present study. Under such a condition, higher levels of in-feed cause diminished diametrical growth but more ovality [18]. On the other hand, for a higher degree of thickness reduction (> 40%), the through-thickness deformation is generally found to be

uniform [19]. A thickness reduction of 35–60% maintained in the present study eliminates the possibility of deformation heterogeneity across the thickness of the tube. Similar results have been obtained by Safari and Joudaki [20]. It has been shown that by increasing the forming increment thickness reduction becomes uniform while fabricating a complicated specimen with a two-point incremental forming process. Due to the higher deformation level, and a relatively smaller clearance between the mandrel and the tube, the in-feed (IF) is believed to exert an almost negligible effect in developing cylindricity error. However, adequate caution must be exercised in choosing a higher deformation level. Although cylindricity is relatively insensitive to the level of the in-feed, it can cause uneven thickness variation as demonstrated by Tabatabaei et al. [21] during bulge forming of tubes utilizing several aluminum alloys. The cylindricity error is a combined effect of diametrical growth, out of roundness or ovality, and straightness of the tube. If the feed-speed ratio is increased, the value of diametrical growth is reduced but the value of ovality increases [11, 22]. So, FS is having a mixed effect on cylindricity error. For the starting and higher ranges, its effect on cylindricity error is opposite to the middle range. This is further corroborated by the results reported by Wang et al. [23] who have studied the spinning stability as a function of the process parameters. It has been found that the increase in the feed rate causes a decrease in the equivalent plastic strain and it is predicted that a larger or smaller feed rate than the optimum one will result in excessive diameter expansion. For the present stagger flow forming experiments, three rollers are positioned 120° apart to balance the forces on the mandrel and to balance the forces acting on it. The positioning of the 3 rollers axially depends on the roller geometry and in-feed for a particular pass to avoid any kind of overlapping zone between rollers. The axial stagger reported for the present study is the axial distance between the first and the third roller. Both the ovality and diametrical growth increase with the increase in AS [15, 15]. Higher levels of axial stagger induce a higher localized bending effect and cause straightness error between 2 extreme rollers. So, axial stagger is having maximum influence in creating cylindricity error in a flow-formed tube. Axial stagger is selected based on the

Table 5 Results of confirmation test of the Regression Model and Optimization

Experiments	FS (mm/Rev)	AS (mm)	IF (mm)	Predicted Results(mm)	Experimental Results (mm)	Error(%)
Regression1 (Intermediate point)	0.75	12.0	4.2	0.276	0.241	12.6
Regression2 (Intermediate point)	0.65	10.0	3.2	0.225	0.255	13.3
GA	0.8	12.0	3.0	0.104	0.096	7.6
TLBO	0.8000	9.516	3.005	0.105	0.096	8.5

value of roller angle and in-feed. In-feed has a lesser influence on cylindricity error. The production rate of the flow formed tube can be increased by increasing in-feed while maintaining the axial stagger in the lesser sensitive range. Cylindricity error can be reduced by reducing axial stagger by changing the roller entry angle along with the increase in the in-feed level.

Confirmation tests have been conducted to validate the regression model, and also optimization values. The results of the confirmation tests have been tabulated in Table 5. Confirmation tests show a good match with predicted results. Hence, it can be inferred from the present analysis that the response equation (Eq. 10) for estimation of cylindricity in terms of three input parameters (FS, AS, IF) can be effectively used to predict the cylindricity error of the flow formed tubes within the parametric range used here.

4 Conclusions

The correlation between the input variables (i.e., feed-speed ratio, axial stagger, and in-feed) and cylindricity of flow formed H30 aluminum tubes has been experimentally determined and modeled using regression analysis. The adequacy of the proposed model has further been analyzed and validated through the confirmation tests. It has been established that the cylindricity error of flow formed tubes increases sharply with an increase in axial stagger (AS). It alone contributes 39% to the cylindricity error, whereas the percentage contributions of in-feed and feed-speed ratio are found to be less than 1%. The regression model developed to establish the relationship between cylindricity error, and the input variable shows a good fit with respect to the experimental data. The model has further been validated with forming trials employing intermediate levels of processing parameters. The interaction terms of FS, AS and IF contribute around another 45%.

Further, 2 meta-heuristic optimization algorithms have been employed to optimize the multivariate processing parameters so as to obtain a global minimum of the cylindricity value. It has been found that the results of the optimization study using both TLBO and GA concepts yield similar results. The optimized levels of processing parameters have been validated by confirmation tests. The results show a close match of about 8%.

The present study establishes that a combination of higher feed rate and lower value of axial stagger and in-feed parameters is essential to achieve the lowest cylindricity error in H30 Al alloy tube by flow forming.

However, the present study is concerned with the optimization and validation of the input processing parameters within a selected range for producing defect-free flow form tube with the minimum cylindricity error. In the

future, the model may be validated for a more wide range of processing parameters and various materials, especially those having deformation characteristics different than the present alloy.

Acknowledgements The authors wish to acknowledge the financial support from the Defence Research and Development Organization (DRDO), Government of India. Authors also acknowledge the Directors of respective organizations (ASL, DRDL, DMRL, and NIT Durgapur) for granting permission to carry out and publish this research work.

Compliance with ethical standards

Conflict of Interest The authors declare that they have no conflict of interest.

Open Access This article is licensed under a Creative Commons Attribution 4.0 International License, which permits use, sharing, adaptation, distribution and reproduction in any medium or format, as long as you give appropriate credit to the original author(s) and the source, provide a link to the Creative Commons licence, and indicate if changes were made. The images or other third party material in this article are included in the article's Creative Commons licence, unless indicated otherwise in a credit line to the material. If material is not included in the article's Creative Commons licence and your intended use is not permitted by statutory regulation or exceeds the permitted use, you will need to obtain permission directly from the copyright holder. To view a copy of this licence, visit <http://creativecommons.org/licenses/by/4.0/>.

References

1. Kalpakjian S, Rajagopal S (1982) Spinning of tubes: a review. *J Appl Metal Working* 2(3):211–223. <https://doi.org/10.1007/BF02834039>
2. Cheraghi SH, Jiang G, Ahmad JS (2003) Evaluating the geometric characteristics of cylindrical features. *Precision Engineering* 27(2):195–204. [https://doi.org/10.1016/S0141-6359\(02\)00221-0](https://doi.org/10.1016/S0141-6359(02)00221-0)
3. Alrazzaq MA, Ahmed M, Younes M (2018) Experimental investigation on geometrical accuracy of CNC multipass sheet metal spinning process. *J Manuf Mater Process* 2(3):59. <https://doi.org/10.3390/jmmp2030059>
4. Song X, Fong KS, Oon SR, Tiong WR, Li PF, Korsunsky AM, Danno A (2014) Diametrical growth in forward flow forming process, simulation, validation and prediction. *Int J Adv Manuf Technol* 71:207–217. <https://doi.org/10.1007/s00170-013-5492-x>
5. Davidson MJ, Balasubramanian K, Tagore GRN (2008) An experimental study on the quality of flow-formed AA6061 tubes. *J Mater Process Technol* 203(1–3):321–325. <https://doi.org/10.1016/j.jmatprotec.2007.10.021>
6. Ebrahimi M, Tabei KH, Naseri R, Djavanroodi F (2017) Effect of flow forming parameters on surface quality geometrical precision and mechanical properties of titanium tube. *J Process Mech Eng.* 232(6):702–708. <https://doi.org/10.1177/0954408917738126>
7. Podder B, Banerjee P, Kumar RK, Hui NB (2019) Study of the influences of process parameters on cold flow forming of Al-tubes. *Int J Mod Manuf Technol* 11(1):95–106

8. Deb K, Anand A, Joshi D (2002) A computationally efficient evolutionary algorithm for real-parameter optimization. *Evolutionary Comput* 10(4):371–395. <https://doi.org/10.1162/106365602760972767>
9. Rao RV (2016) Review of applications of TLBO algorithm and a tutorial for beginners to solve the unconstrained and constrained optimization problems. *Decis Sci Lett* 5:1–30. <https://doi.org/10.5267/j.dsl.2015.9.003>
10. Huang Z, Dantan TY, Etienne A, Rivette M, Bonnet N (2017) Geometrical deviation identification and prediction method for additive manufacturing. *Rapid Prototyp J* 24(9):1524–1538. <https://doi.org/10.1108/RPJ-07-2017-0137>
11. Podder B, Mondal C, Ramesh Kumar K, Yadav DR (2012) Effect of preform heat treatment on the flow formability and mechanical properties of AISI 4340 steel. *Mater Des* 37:174–181
12. Bhatt JB, Bhatt RJ, Raval HK, Desai KP (2021) Effect of operating parameters on forces during backward flow forming process for AA6061. In: Nedelcu D, Dave HK (eds) *Advances in Manufacturing Processes*. Lecture Notes in Mechanical Engineering. Springer, Singapore
13. Dimensioning and Tolerancing (1994) American Society of Mechanical Engineers, ANSI Y14.5, New York.
14. Ashok SD, Samuel GL (2011) Least square curve fitting technique for processing time sampled high speed spindle data. *Int J Manuf Res* 6(3):256–276. <https://doi.org/10.1504/IJMR.2011.041129>
15. Rao RV (2016) *Teaching learning based optimization algorithm*, 1st edn. Springer international Publishing, Switzerland
16. Rao RV, Kalyankar VD (2013) Multipass turning process parameter optimization using teaching-learning-based optimization algorithm. *Scientia Iranica* 20(3):967–974. <https://doi.org/10.1016/j.scient.2013.01.002>
17. Goldberg DE (1988) *Genetic algorithms in search, optimisation, and machine learning*. Genetic AI, Proceedings, Addison-Wesley Longman Publishing Co. Boston, MA.
18. Srinivasulu M, Komaraiah M, Rao CSKP (2012) Experimental investigations to predict mean diameter of AA6082 tube in flow forming process—a DOE approach. *IOSR J Eng* 2(6):52–60
19. Gur M, Tirosh J (1982) Plastic flow instability under compressive loading during shear spinning process. *J Eng for Industry* 104(1):17–22. <https://doi.org/10.1115/1.3185791>
20. Safari M, Joudaki J (2019) Fabrication of a complicated specimen with two point incremental forming process. *Int J Adv Des Manufac Technol* 12(4):83–88
21. Tabatabaei SM, Dehkordi RK, Safari M (2019) Cold bulge forming of aluminum tubes: effects of geometrical and process parameters on formability and thickness variation in bulged tubes. *Trans Indian Inst Met* 72(6):2649–2661. <https://doi.org/10.1007/s12666-019-01733-w>
22. Srinivasulu M, Komaraiah M, Krishna RSKP (2012) Experimental studies on the characteristics of AA6082 flow formed tubes. *J Mech Eng Res* 4(6):192–198. <https://doi.org/10.5897/JMER11.063>
23. Wang C, Wu J, Chen J, Xiang Z, Sheng X (2020) Stability research on spinning of ultra-thin-wall aluminum alloy tube. *SN Appl Sci* 2:941. <https://doi.org/10.1007/s42452-020-2752-x>
24. Marini D (2016) Flow forming: A review of research methodologies, prediction models and their applications. *Int J Mech Eng Technol* 7(5):285–315

Publisher's Note Springer Nature remains neutral with regard to jurisdictional claims in published maps and institutional affiliations.